Tuning the Attempt Frequency of Protein Folding Dynamics via Transition-State Rigidification: Application to Trp-Cage

Rachel M. Abaskharon,[†,‖] Robert M. Culik,[‡,‖] G. Andrew Woolley,[§] and Feng Gai*[,†]

[†]Department of Chemistry and [‡]Department of Biochemistry & Biophysics, University of Pennsylvania, 231 South 34th Street, Philadelphia, Pennsylvania 19104, United States

[§]Department of Chemistry, University of Toronto, 80 Saint George Street, Toronto, Ontario M5S 3H6, Canada

Ⓢ *Supporting Information*

ABSTRACT: The attempt frequency or prefactor (k_0) of the transition-state rate equation of protein folding kinetics has been estimated to be on the order of 10^6 s^{-1}, which is many orders of magnitude smaller than that of chemical reactions. Herein we use the mini-protein Trp-cage to show that it is possible to significantly increase the value of k_0 for a protein folding reaction by rigidifying the transition state. This is achieved by reducing the conformational flexibility of a key structural element (i.e., an α-helix) formed in the transition state via photo-isomerization of an azobenzene cross-linker. We find that this strategy not only decreases the folding time of the Trp-cage peptide by more than an order of magnitude (to ~100 ns at 25 °C) but also exposes parallel folding pathways, allowing us to provide, to the best of our knowledge, the first quantitative assessment of the curvature of the transition-state free-energy surface of a protein.
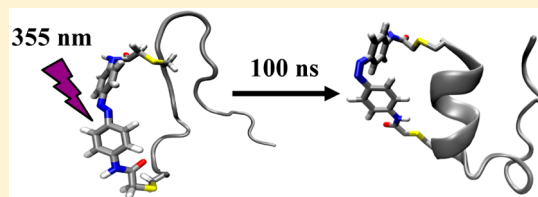
Conformational diffusion on an energy landscape that is biased toward the native state ensures that protein folding is a thermodynamically robust and productive event.[1-4] However, during folding, the free energy of the system does not always show a monotonic decrease; instead, it can increase over a relatively small region of the landscape, leading to the formation of folding free energy barriers. Because these barriers contain key information for achieving a comprehensive understanding of the mechanisms of protein folding, significant efforts have been made to investigate how and why such kinetic bottlenecks are generated as well as the structural characteristics of the associated transition states.[5] More recently, several studies have focused on elucidating the dynamic aspects of the folding free energy barrier, such as the roughness of the underlying free energy surface[6] and the transition path time.[7,8] According to Kramers' theory[9]

$$k = \frac{\omega_R \omega_B}{2\pi\gamma} \exp\left(-\frac{\Delta G^{\neq}}{RT}\right)$$

(1)

where R is the gas constant and T is the absolute temperature, the rate of a barrier-crossing process is determined not only by the height of the barrier ($\Delta G^{\neq}$) but also by the curvatures of the reactant (ω_R^2) and transition-state (ω_B^2) potential wells as well as the friction coefficient (γ). The latter manifests as the roughness of the potential energy surface. While direct experimental assessments of ω_R and ω_B are currently not possible, many previous studies[10,11] have been performed to determine the pre-exponential factor, often referred to as the attempt frequency (k_0). Interestingly, the value of k_0 for protein folding is estimated to be in the range of 10^3 to 10^6 s^{-1},[12] which is several orders of magnitude smaller than that observed for

chemical reactions and thus suggests that the curvature of the protein folding transition-state potential well (i.e., ω_B^2) is intrinsically small. This is consistent with the well-recognized notion that the folding transition state consists of an ensemble of structures that contain only a fraction of the native contacts and hence is inherently flexible. Gas-phase chemical reactions between small molecules often encounter a transition state that contains a single, distinct species in a highly constrained geometric configuration. In this regard, we hypothesize that by rigidifying the folding transition state one could significantly increase ω_B and hence k_0 (eq 1). In this proof-of-concept study, we chose a mini-protein, Trp-cage,[13,14] as our model system and employed an azobenzene cross-linker to modify the curvature of its free-energy barrier.

Trp-cage is one of the most extensively studied model peptide systems in protein folding,[15-54] which has led to a fairly detailed understanding of its folding mechanism. For example, both experimental[22,40,41,48-50] and computational[16-18,23,24,27,30-39,42,44,46,47] studies have shown that the α-helix is either partially or completely formed in the major folding transition state, often without the presence of many native tertiary stabilizing interactions. Thus, this feature provides a unique opportunity to modify the characteristics of the folding transition state of Trp-cage via a photoactivatable cross-linker. As shown (Figure 1), our working hypothesis is that upon imposing a geometric constraint on the Trp-cage α-helix via photoinduced isomerization of an azobenzene cross-
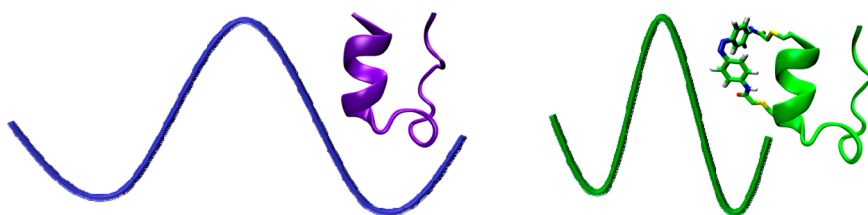
Figure 1. Schematic representation of how the azobenzene cross-linker alters the curvature of the folding free energy surface of Trp-cage.

linker, we will be able to not only initiate folding but also force the conformational search to pass through a more rigidified transition state, thus making the attempt frequency (i.e., k_0) of this folding "reaction" larger.

We chose an amidoazobenzene derivative as the photo-activatable cross-linker based on the fact that (1) its cis isomeric form supports or stabilizes α-helical conformations when attached between the i and $i+7$ positions of a peptide,[55] whereas its trans form does not, (2) its trans form is thermodynamically more favorable (>95%) in the dark at room temperature,[56] (3) upon irradiation with 355 nm light, the trans to cis isomerization occurs on the picosecond time scale,[57] which is significantly faster than the folding time of Trp-cage, and (4) the spontaneous back-reaction, that is, the cis to trans isomerization, takes place on the time scale of minutes at room temperature.[58] Specifically, we introduced the azobenzene moiety into a mutant of the Trp-cage 10b variant containing cysteine substitutions at residues 1 and 8 (sequence: CAYAQWLCDGGPSSGRPPPS), using standard cysteine alkylation methods.[55] As previously indicated, the resultant Trp-cage peptide (hereafter referred to as 10b-azob) should fold only when the azobenzene cross-linker is in its cis isomeric form (Figure 1).

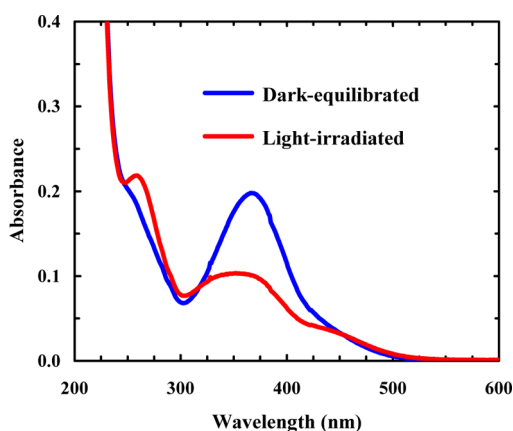As shown (Figure 2), the π–π^* transition of trans-amidoazobenzene at ~367 nm has a significant decrease in

Figure 2. Absorption spectra of dark-equilibrated and light-irradiated 10b-azob peptides (~10 μM), as indicated. The light-irradiated sample was prepared by irradiating the dark-equilibrated sample with 355 nm light (~8.8 mW cm^{-2}) for 5 min.

intensity upon irradiation of 10b-azob with 355 nm light, whereas there is a gain in absorbance at ~258 nm, which corresponds to the π–π^* transition of cis-amidoazobenzene.[55] Furthermore, as expected (Figure 3), the circular dichroism (CD) spectrum of the dark-equilibrated 10b-azob sample (in a 20/80 trifluoroethanol/water mixture) indicates that the peptide adopts mostly disordered conformations, whereas the
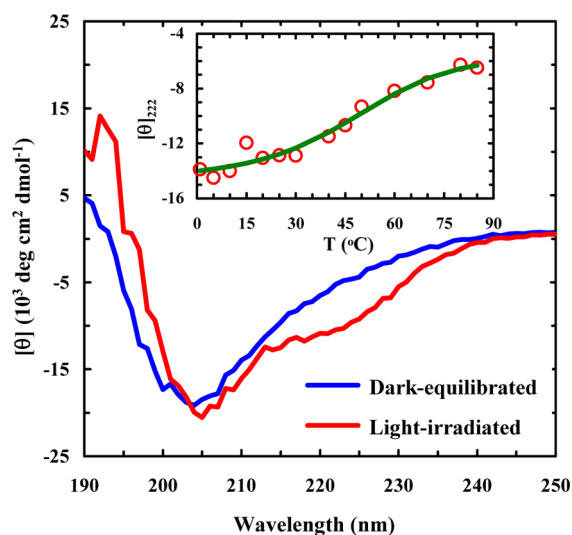

Figure 3. CD spectra of dark-equilibrated and light-irradiated 10b-azob samples (~33 μM in a 20/80 trifluoroethanol/water solution), as indicated. The light-irradiated sample was prepared as described in the caption of Figure 2. Inset: CD T-melt of the light-irradiated 10b-azob sample, monitored at 222 nm. The solid line is a fit of the data to a two-state model using the same thermodynamic parameters determined for the wild-type Trp-cage 10b.[40]

CD spectrum of the light-irradiated sample indicates that light absorption indeed prompts α-helix formation. The reason that we added trifluoroethanol (TFE), which is known to promote α-helix formation,[59] is that in pure water the light-irradiated peptide exhibits relatively low helicity. This is most likely due to the fact that addition of the azobenzene cross-linker eliminates the favorable N-terminal helical cap, which has been shown to be detrimental to the stability of Trp-cage.[60,61] More importantly, in the presence of 20% TFE the CD signal of the light-irradiated 10-azob sample at 222 nm shows a similar sigmoidal dependence on temperature as that of the wild-type peptide (Figure 3, inset), suggesting that the peptide's cage structure is formed when the azobenzene moiety is in its cis form and that the addition of TFE compensates for the loss of helix stability upon cross-linking. The latter is supported by the fact that addition of 20% TFE only leads to a small increase (~7 °C) in the thermal melting temperature of Trp-cage 10b (Supporting Information).

The light-induced folding kinetics of 10b-azob were probed using a time-resolved infrared (IR) apparatus.[62] Briefly, the 355 nm pump pulse (3−5 ns) was derived from a Minilite II Nd:YAG laser (Continuum, CA), and a tunable 1001-TLC quantum cascade (QC) laser (Daylight Solutions, CA) was used as the continuous-wave (CW) IR probe. As indicated (Figure 4), the light-induced conformational dynamics of 10b-azob at 25 °C, probed at 1630 cm^{-1} where helical content is known to absorb,[63] show an increase in absorbance as a
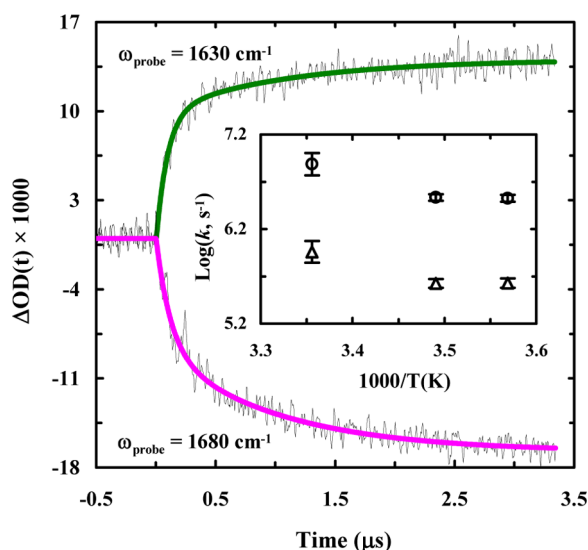
Figure 4. Conformational kinetics of 10b-azob (in a 20/80 trifluoroethanol/water solution) induced by a nanosecond 355 nm laser pulse and probed at different frequencies, as indicated. These kinetic traces were collected at 25 °C and in each case a linear and instrument-limited signal arising from the solvent due to the pump-induced temperature jump (~1 °C) has been subtracted for clarity. The smooth lines are fits of these traces to a double-exponential function with the following time constants (relative percentages): 90 ± 20 ns (74%) and 1100 ± 100 ns (26%) for 1630 cm^{-1} and 120 ± 20 ns (54%) and 1000 ± 90 ns (46%) for 1680 cm^{-1}. Inset: Temperature dependence of the fast and slow rate constants of 10b-azob obtained at 1630 cm^{-1}.

cross-linked peptide that corresponds to the Trp-cage 10b α-helix (sequence: CAYAQWLCD, hereafter referred to as 10b-h-azob). As indicated (Figure 5), the light-induced kinetics of
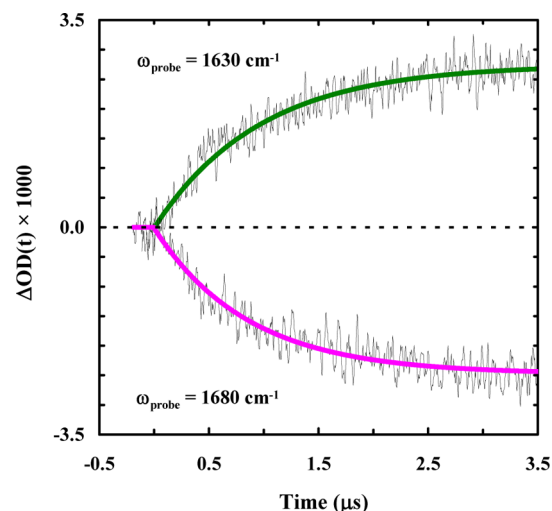

Figure 5. Conformational kinetics of 10b-h-azob (in a 20/80 trifluoroethanol/water solution) induced by a nanosecond 355 nm laser pulse and probed at different frequencies, as indicated. These kinetic traces were collected at 24.4 °C, and in each case a linear background signal arising from the solvent has been subtracted for clarity. The smooth lines are fits of these traces to a single-exponential function with the following time constants: 960 ± 60 ns for 1630 cm^{-1} and 860 ± 40 ns for 1680 cm^{-1}.

function of time, consistent with the CD results (Figure 3). What is more interesting, however, is that this kinetic trace is best fit to a double-exponential with time constants that differ by an order of magnitude (i.e., 90 ns versus 1.1 μs). Further measurements at 1680 cm^{-1}, where disordered conformations have a larger absorbance, show identical results (Figure 4). Previously, we have shown that the folding time of Trp-cage 10b is ~1.6 μs at 25 °C.[40] Thus, the slower kinetic phase in the current case is similar to the folding kinetics of the wild type peptide, whereas the faster kinetic phase represents a previously unobserved folding event. Taken together, these results indicate that by photoinitiating isomerization of an azobenzene cross-linker added to the α-helical segment of the Trp-cage sequence, we are creating either two parallel pathways that have distinctly different folding rates or a sequential pathway that involves a folding intermediate.

It has recently been shown that the 3$_{10}$-helix of Trp-cage 10b folds on the order of hundreds of nanoseconds and the formation of this structure is considered to be the last step in the folding process.[40] However, it is unlikely that the fast component seen in these experiments comes from 3$_{10}$-helix formation for two reasons. First, 3$_{10}$-helices typically absorb in the 1660 cm^{-1} region,[64] yet the ~100 ns component observed for 10b-azob is detected at both 1630 and 1680 cm^{-1}. Also, the 3$_{10}$-helix of Trp-cage 10b is relatively unstable and, as a result, the previous study[40] was only able to detect its folding–unfolding kinetics at temperatures below ~20 °C. Another possibility is that the fast phase reports on the formation of an intermediate state that contains a native or native-like α-helix, which goes on to form the folded Trp-cage structure with a slower folding rate. To test this possibility, we studied the photoinduced conformational dynamics of another azobenzene

10b-h-azob in the presence of 20% TFE, probed at 1630 and 1680 cm^{-1}, can be described by a single-exponential function, with a time constant of ~1.0 μs for both cases. This result is consistent with the study of Serrano et al.,[65] which showed that the folding time of a helical peptide with a side chain–side chain cross-linker is on the order of 1 μs. Perhaps most importantly, our 10b-h-azob results are in line with those of Hamm and coworkers,[66] who observed that the presence of an azobenzene cross-linker in a short α-helical peptide acts as a thermodynamic constraint rather than a dynamic one. In this regard, they observed that rather than initiating a fast downhill folding process, the azobenzene photoswitch allowed for the stabilization of metastable, non-native free-energy traps. Therefore, these results prompt us to conclude that the fast (i.e., ~100 ns) component seen in the case of 10b-azob does not arise from an early, partially folded, on-pathway Trp-cage intermediate wherein only the α-helix is formed; instead, it corresponds to an alternative but much faster folding pathway. Similarly, a sequential scenario in which the α-helix is formed in ~1 μs followed by a 100 ns folding event can also be ruled out, as the current experimental strategy is unable to detect a fast kinetic event following a slower one. Moreover, these kinetic results also argue against the idea that the faster folding component of 10b-azob results from a decrease in the folding free energy barrier, as we would expect similar double-exponential behavior for 10b-h-azob in this case. This is because, as previously discussed, the rate-limiting step in Trp-cage folding corresponds to helix formation. Thus, tertiary interactions with the rest of the 10b-azob peptide seem to play an influential role in creating this alternate protein folding pathway. Indeed, kinetic measurements carried out on 10b-azob at different temperatures reveal that both rates have very similar dependences on temperature (Figure 4, inset), further

supporting the idea that the azobenzene cross-linker is not affecting the free-energy barrier height but rather altering the frequency with which the system leaves the transition state region.

In summary, because an additional parallel pathway originating from the same reactant can only lead to an increase in the overall reaction rate, our interpretation implies, as shown in the following kinetic scheme, that upon photoisomerization of the azobenzene cross-linker two distinguishable conformational ensembles ($U_{1,cis}$ and $U_{2,cis}$) in the unfolded potential well of 10b-azob are rapidly formed
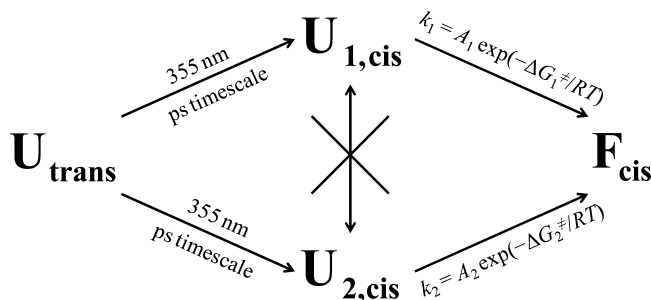
where $A_1 \approx 10A_2$, $\Delta G_1^{\neq} \approx \Delta G_2^{\neq}$, and the exchange rate between $U_{1,cis}$ and $U_{2,cis}$ is significantly slower than their folding rates to form F_{cis}. Also of note, both k_1 and k_2 are significantly faster than the single-exponential folding rate (τ_F is in the range of 5–7 μs) of another cross-linked Trp-cage peptide.[61] It was shown previously that when a helix cross-linker, m-xylene, was placed between positions 4 and 8 of the Trp-cage 10b sequence, both the folding and unfolding rates of the resultant peptide were significantly decreased in comparison with those of the wild-type Trp-cage 10b.[61,67] This was attributed to a frictional effect of m-xylene, as it was located at the most sterically congested region of the peptide. Because the azobenzene cross-linker is not only longer but also more flexible than m-xylene, it is expected to cause a much smaller perturbation due to internal friction. In addition, in keeping with the present hypothesis, the findings obtained with the m-xylene cross-linker suggest that crossing-linking a single α-helical turn is insufficient to significantly increase the rigidity of the folding transition state.

The notion that the two kinetic phases of 10b-azob arise from parallel folding pathways that have identical or comparable free energy barriers suggests that we could further estimate the value of ω_B, which, to the best of our knowledge, has never been done before. On the basis of eq 1, it is easy to show that

$$\frac{k_S}{k_F} = \frac{\omega_{BS}}{\omega_{BF}} \tag{2}$$

assuming that ω_R for both the fast and slow pathways is the same, where k_S and k_F are the rate constants of the slow and fast components, respectively, while ω_{BS} and ω_{BF} are the frequencies of the respective transition-state harmonic potential wells. In turn, these frequencies determine the free energy (G_B) of motion along the folding coordinate (q) near the transition state

$$G_B = \Delta G^{\neq} - \frac{1}{2}m\omega_B^2 q^2 \tag{3}$$

where m is the effective mass of the particle. Following eq 3, one can easily show that for the same displacement along the folding coordinate, that is, Δq, the free-energy difference between the two aforementioned harmonic wells would be

$$\Delta G_B = \frac{1}{2}m(\omega_{BF}^2 - \omega_{BS}^2)(\Delta q)^2 \tag{4}$$

Thus, by combining eqs 2 and 4 and using the experimentally determined values of k_S and k_F, one could solve for ω_{BS} and ω_{BF} if ΔG_B and Δq are known. Whereas both are difficult, if not impossible, to be determined, we can make reasonable estimates in the current case. As previously concluded, the fast folding phase arises from a more rigid transition state. In other words, it is the entropic effect of the azobenzene cross-linker that makes ω_{BF} larger. Using the values for change in conformational entropy upon helix formation determined by Hofrichter et al.,[68] we estimated the maximum entropic stabilization of helical structure arising from the azobenzene cross-linker to be ~6 kcal/mol. By further assuming that the peptide, which has a molecular weight of 2049.2 g/mol, needs to move a distance that is one-fourth of the radius of gyration of Trp-cage to cross the transition state, or $\Delta q = 3$ Å,[23] we found that $\omega_{BS} = 5.24 \times 10^{10}$ rad/s. This estimate provides what, to the best of our knowledge, is the first experimental assessment of the frequency of the protein folding transition state. By further assuming that ω_R is on the same order of magnitude as ω_B, an assumption commonly used in the literature,[10,12] and $D = 10^{-6}$ cm²/s as an upper limit,[69] we estimated k_0 to be 6.9×10^6 s^{-1} for the folding kinetics of the unconstrained Trp-cage peptide.

Despite its approximate nature, the previous calculation yields a k_0 value that is in good agreement with previously estimated values based on measurements of the folding rate of ultrafast folders[11] and the rate of contact formation in unfolded protein ensembles[70] as well as those based on simulations[10] and theoretical predictions.[71] In particular, this value compares well with that ($10^{7\pm1}$ s^{-1}) determined by Yu et al.,[8] who used single-molecule force spectroscopy to characterize the folding free-energy landscape and rate of a prion protein. Therefore, these agreements provide further support, albeit indirectly, of our interpretation and analysis of the kinetics results obtained with 10b-azob.

Although all of the evidence supports the aforementioned folding mechanism of 10b-azob, it is worth mentioning that an alternative interpretation for the observed nonexponential behavior is due to projection of the protein onto an incipient downhill folding landscape upon azobenzene isomerization. Gruebele and coworkers[72,73] have found that under certain conditions proteins can be engineered to fold in a complex manner, in which there is both a slow phase due to some molecules diffusing on a landscape containing a barrier (activated folding) and a fast phase resulting from other molecules navigating a barrierless landscape (downhill folding). We have tentatively ruled out this possibility based on the kinetic results of 10b-h-azob (Figure 5) and the similar temperature dependence of the fast and slow rate constants of 10b-azob (Figure 4).

While extensive effort has gone into identifying the structures of folding transition states of peptides and proteins, aside from the ability to further stabilize these proteins and to obtain generic protein design strategies, there have not been many examples of using this knowledge to actively change the nature of a protein's folding, for example, altering the shape of the protein folding free-energy barrier. Here we show, using Trp-cage as a testbed, that it is possible to tune the attempt frequency of protein folding dynamics via rigidification of the transition state. Specifically, we exploit the trans to cis

isomerization of an azobenzene cross-linker via phototriggering to not only initiate folding but also provide a certain degree of constraint on the conformational flexibility of the α-helix of Trp-cage, which has previously been shown to be formed in the transition state. Transient IR measurements reveal that this strategy produces biphasic kinetics of folding, with time constants that differ by an order of magnitude (i.e., 100 ns versus 1 μs). Further control experiments on a truncate of Trp-cage containing just the α-helix segment provide strong evidence indicating that the fast kinetic phase does not arise from an intermediate; instead, it is confirmation of a parallel folding pathway whose transition-state potential well has a larger curvature in comparison with that of the wild-type Trp-cage. Moreover, from these experimental results, we are able to estimate the frequency of the transition state of Trp-cage to be on the order of 10^{10} rad/s.

■ ASSOCIATED CONTENT

Ⓢ Supporting Information

Experimental methods and a CD *T*-melt of Trp-cage 10b in a 20/80 trifluoroethanol/water. This material is available free of charge via the Internet at http://pubs.acs.org.

■ AUTHOR INFORMATION

Corresponding Author
*E-mail: gai@sas.upenn.edu.

Author Contributions
‖R.M.A. and R.M.C. contributed equally to this work.

Notes
The authors declare no competing financial interest.

■ ACKNOWLEDGMENTS

■ REFERENCES

(1) Chan, H. S.; Dill, K. A. Protein Folding in the Landscape Perspective: Chevron Plots and Non-Arrhenius Kinetics. *Proteins: Struct., Funct., Genet.* **1998**, *30*, 2−33.

(2) Goldbeck, R. A.; Thomas, Y. G.; Chen, E.; Esquerra, R. M.; Kliger, D. S. Multiple Pathways on a Protein-Folding Energy Landscape: Kinetic Evidence. *Proc. Natl. Acad. Sci. U. S. A.* **1999**, *96*, 2782−2787.

(3) Bryngelson, J. D.; Wolynes, P. G. Spin Glasses and the Statistical Mechanics of Protein Folding. *Proc. Natl. Acad. Sci. U. S. A.* **1987**, *84*, 7524−7528.

(4) Leopold, P. E.; Montal, M.; Onuchic, J. N. Protein Folding Funnels: A Kinetic Approach to the Sequence-Structure Relationship. *Proc. Natl. Acad. Sci. U. S. A.* **1992**, *89*, 8721−8725.

(5) Matouschek, A.; Kellis, J. T.; Serrano, L.; Fersht, A. R. Mapping the Transition State and Pathway of Protein Folding by Protein Engineering. *Nature* **1989**, *340*, 122−126.

(6) Liu, F.; Nakaema, M.; Gruebele, M. The Transition State Transit Time of WW Domain Folding is Controlled by Energy Landscape Roughness. *J. Chem. Phys.* **2009**, *131*, 195101.

(7) Chung, H. S.; Eaton, W. A. Single-Molecule Fluorescence Probes Dynamics of Barrier Crossing. *Nature* **2013**, *502*, 685−688.

(8) Yu, H.; Gupta, A. N.; Liu, X.; Neupane, K.; Brigley, A. M.; Sosova, I.; Woodside, M. T. Energy Landscape Analysis of Native Folding of the Prion Protein Yields the Diffusion Constant, Transition Path Time, and Rates. *Proc. Natl. Acad. Sci. U. S. A.* **2012**, *109*, 14452−14457.

(9) Hänggi, P.; Borkovec, M. Reaction-Rate Theory: Fifty Years After Kramers. *Rev. Mod. Phys.* **1990**, *62*, 251−341.

(10) Best, R.; Hummer, G. Diffusive Model of Protein Folding Dynamics with Kramers Turnover in Rate. *Phys. Rev. Lett.* **2006**, *96*, 228104.

(11) Kubelka, J.; Chiu, T. K.; Davies, D. R.; Eaton, W. A.; Hofrichter, J. Sub-microsecond Protein Folding. *J. Mol. Biol.* **2006**, *359*, 546−553.

(12) Schuler, B.; Lipman, E. A.; Eaton, W. A. Probing the Free-Energy Surface for Protein Folding with Single-Molecule Fluorescence Spectroscopy. *Nature* **2002**, *419*, 743−747.

(13) Neidigh, J. W.; Fesinmeyer, R. M.; Andersen, N. H. Designing a 20-Residue Protein. *Nat. Struct. Biol.* **2002**, *9*, 425−430.

(14) Barua, B.; Lin, J. C.; Williams, V. D.; Kummler, P.; Neidigh, J. W.; Andersen, N. H. The Trp-cage: Optimizing the Stability of a Globular Miniprotein. *Protein Eng., Des. Sel.* **2008**, *21*, 171−185.

(15) Qiu, L.; Pabit, S. A.; Roitberg, A. E.; Hagen, S. J. Smaller and Faster: The 20-Residue Trp-Cage Protein Folds in 4 μs. *J. Am. Chem. Soc.* **2002**, *124*, 12952−12953.

(16) Snow, C. D.; Zagrovic, B.; Pande, V. S. The Trp Cage: Folding Kinetics and Unfolded State Topology via Molecular Dynamics Simulations. *J. Am. Chem. Soc.* **2002**, *124*, 14548−14549.

(17) Chowdhury, S.; Lee, M. C.; Xiong, G.; Duan, Y. Ab initio Folding Simulation of the Trp-cage Mini-protein Approaches NMR Resolution. *J. Mol. Biol.* **2003**, *327*, 711−717.

(18) Nikiforovich, G. V.; Andersen, N. H.; Fesinmeyer, R. M.; Frieden, C. Possible Locally Driven Folding Pathways of TC5b, a 20-Residue Protein. *Proteins* **2003**, *52*, 292−302.

(19) Pitera, J. W.; Swope, W. Understanding Folding and Design: Replica-Exchange Simulations of "Trp-cage" Miniproteins. *Proc. Natl. Acad. Sci. U. S. A.* **2003**, *100*, 7587−7592.

(20) Zhou, R. Trp-cage: Folding Free Energy Landscape in Explicit Water. *Proc. Natl. Acad. Sci. U. S. A.* **2003**, *100*, 13280−13285.

(21) Chowdhury, S.; Lee, M. C.; Duan, Y. Characterizing the Rate-Limiting Step of Trp-Cage Folding by All-Atom Molecular Dynamics Simulations. *J. Phys. Chem. B* **2004**, *108*, 13855−13865.

(22) Ahmed, Z.; Beta, I. A.; Mikhonin, A. V.; Asher, S. A. UV-Resonance Raman Thermal Unfolding Study of Trp-cage Shows That It Is Not a Simple Two-State Miniprotein. *J. Am. Chem. Soc.* **2005**, *127*, 10943−10950.

(23) Ding, F.; Buldyrev, S. V.; Dokholyan, N. V Folding Trp-cage to NMR Resolution Native Structure Using a Coarse-Grained Protein Model. *Biophys. J.* **2005**, *88*, 147−155.

(24) Linhananta, A.; Boer, J.; MacKay, I. The Equilibrium Properties and Folding Kinetics of an All-Atom Go Model of the Trp-cage. *J. Chem. Phys.* **2005**, *122*, 114901.

(25) Neuweiler, H.; Doose, S.; Sauer, M. A Microscopic View of Miniprotein Folding: Enhanced Folding Efficiency Through Formation of an Intermediate. *Proc. Natl. Acad. Sci. U. S. A.* **2005**, *102*, 16650−16655.

(26) Bunagan, M. R.; Yang, X.; Saven, J. G.; Gai, F. Ultrafast Folding of a Computationally Designed Trp-cage Mutant: Trp2-cage. *J. Phys. Chem. B* **2006**, *110*, 3759−3763.

(27) Chen, J.; Im, W.; Brooks, C. L. Balancing Solvation and Intramolecular Interactions: Toward a Consistent Generalized Born Force Field. *J. Am. Chem. Soc.* **2006**, *128*, 3728−3736.

(28) Juraszek, J.; Bolhuis, P. G. Sampling the Multiple Folding Mechanisms of Trp-cage in Explicit Solvent. *Proc. Natl. Acad. Sci. U. S. A.* **2006**, *103*, 15859−15864.

(29) Fedorov, D. G.; Kitaura, K. Extending the Power of Quantum Chemistry to Large Systems with the Fragment Molecular Orbital Method. *J. Phys. Chem. B* **2007**, *111*, 6904−6914.

(30) Kentsis, A.; Gindin, T.; Mezei, M.; Osman, R. Calculation of the Free Energy and Cooperativity of Protein Folding. *PloS One* **2007**, *2*, e446.

(31) Paschek, D.; Nymeyer, H.; García, A. E. Replica Exchange Simulation of Reversible Folding/Unfolding of the Trp-cage Miniprotein in Explicit Solvent: On the Structure and Possible Role of Internal Water. *J. Struct. Biol.* **2007**, *157*, 524−533.

(32) Piana, S.; Laio, A. A Bias-Exchange Approach to Protein Folding. *J. Phys. Chem. B* **2007**, *111*, 4553−4559.

(33) Yang, L.; Grubb, M. P.; Gao, Y. Q. Application of the Accelerated Molecular Dynamics Simulations to the Folding of a Small Protein. *J. Chem. Phys.* **2007**, *126*, 125102.

(34) Juraszek, J.; Bolhuis, P. G. Rate Constant and Reaction Coordinate of Trp-cage Folding in Explicit Water. *Biophys. J.* **2008**, *95*, 4246−4257.

(35) Paschek, D.; Hempel, S.; García, A. E. Computing the Stability Diagram of the Trp-cage Miniprotein. *Proc. Natl. Acad. Sci. U. S. A.* **2008**, *105*, 17754−17759.

(36) Xu, W.; Mu, Y. Ab Initio Folding Simulation of Trpcage by Replica Exchange with Hybrid Hamiltonian. *Biophys. Chem.* **2008**, *137*, 116−125.

(37) Černý, J.; Vondrášek, J.; Hobza, P. Loss of Dispersion Energy Changes the Stability and Folding/Unfolding Equilibrium of the Trp-Cage Protein. *J. Phys. Chem. B* **2009**, *113*, 5657−5660.

(38) Marinelli, F.; Pietrucci, F.; Laio, A.; Piana, S. A Kinetic Model of Trp-Cage Folding from Multiple Biased Molecular Dynamics Simulations. *PLoS Comput. Biol.* **2009**, *5*, e1000452.

(39) Best, R. B.; Mittal, J. Balance Between Alpha and Beta Structures in Ab Initio Protein Folding. *J. Phys. Chem. B* **2010**, *114*, 8790−8798.

(40) Culik, R. M.; Serrano, A. L.; Bunagan, M. R.; Gai, F. Achieving Secondary Structural Resolution in Kinetic Measurements of Protein Folding: A Case Study of the Folding Mechanism of Trp-cage. *Angew. Chem., Int. Ed.* **2011**, *50*, 10884−10887.

(41) Hałabis, A.; Żmudzińska, W.; Liwo, A.; Ołdziej, S. Conformational Dynamics of the Trp-Cage Miniprotein at Its Folding Temperature. *J. Phys. Chem. B* **2012**, *116*, 6898−6907.

(42) Shao, Q.; Shi, J.; Zhu, W. Enhanced Sampling Molecular Dynamics Simulation Captures Experimentally Suggested Intermediate and Unfolded States in the Folding Pathway of Trp-cage Miniprotein. *J. Chem. Phys.* **2012**, *137*, 125103.

(43) Byrne, A.; Kier, B. L.; Williams, D. V.; Scian, M.; Andersen, N. H. Circular Permutation of the Trp-cage: Fold Rescue upon Addition of a Hydrophobic Staple. *RSC Adv.* **2013**, *2013*, 19824−19829.

(44) Juraszek, J.; Saladino, G.; Van Erp, T.; Gervasio, F. Efficient Numerical Reconstruction of Protein Folding Kinetics with Partial Path Sampling and Pathlike Variables. *Phys. Rev. Lett.* **2013**, *110*, 108106.

(45) Lai, Z.; Preketes, N. K.; Mukamel, S.; Wang, J. Monitoring the Folding of Trp-cage Peptide by Two-Dimensional Infrared (2DIR) Spectroscopy. *J. Phys. Chem. B* **2013**, *117*, 4661−4669.

(46) Lee, I.-H.; Kim, S.-Y. Dynamic Folding Pathway Models of the Trp-cage Protein. *BioMed. Res. Int.* **2013**, *2013*, 973867.

(47) Marinelli, F. Following Easy Slope Paths on a Free Energy Landscape: The Case Study of the Trp-cage Folding Mechanism. *Biophys. J.* **2013**, *105*, 1236−1247.

(48) Meuzelaar, H.; Marino, K. A.; Huerta-Viga, A.; Panman, M. R.; Smeenk, L. E. J.; Kettelarij, A. J.; Van Maarseveen, J. H.; Timmerman, P.; Bolhuis, P. G.; Woutersen, S. Folding Dynamics of the Trp-cage Miniprotein: Evidence for a Native-Like Intermediate from Combined Time-Resolved Vibrational Spectroscopy and Molecular Dynamics Simulations. *J. Phys. Chem. B* **2013**, *117*, 11490−11501.

(49) Rovó, P.; Stráner, P.; Láng, A.; Bartha, I.; Huszár, K.; Nyitray, L.; Perczel, A. Structural Insights into the Trp-cage Folding Intermediate Formation. *Chem.—Eur. J.* **2013**, *19*, 2628−2640.

(50) Byrne, A.; Williams, D. V.; Barua, B.; Hagen, S. J.; Kier, B. L.; Andersen, N. H. Folding Dynamics and Pathways of the Trp-Cage Miniproteins. *Biochemistry* **2014**, *53*, 6011−6021.

(51) Doshi, U.; Hamelberg, D. Achieving Rigorous Accelerated Conformational Sampling in Explicit Solvent. *J. Phys. Chem. Lett.* **2014**, *5*, 1217−1224.

(52) Du, W.; Bolhuis, P. G. Sampling the Equilibrium Kinetic Network of Trp-cage in Explicit Solvent. *J. Chem. Phys.* **2014**, *140*, 195102.

(53) Kannan, S.; Zacharias, M. Role of Tryptophan Side Chain Dynamics on the Trp-cage Mini-Protein Folding Studied by Molecular Dynamics Simulations. *PloS One* **2014**, *9*, e88383.

(54) Mou, L.; Jia, X.; Gao, Y.; Li, Y.; Zhang, J. Z. H.; Mei, Y. Folding Simulation of Trp-cage Utilizing a New AMBER Compatible Force Field with Coupled Main Chain Torsions. *J. Theor. Comput. Chem.* **2014**, *13*, 1450026.

(55) Kumita, J. R.; Smart, O. S.; Woolley, G. A. Photo-control of Helix Content in a Short Peptide. *Proc. Natl. Acad. Sci. U. S. A.* **2000**, *97*, 3803−3808.

(56) Renner, C.; Behrendt, R.; Spörlein, S.; Wachtveitl, J.; Moroder, L. Photomodulation of Conformational States. I. Mono- and Bicyclic Peptides with (4-Amino)phenylazobenzoic Acid as Backbone Constituent. *Biopolymers* **2000**, *54*, 489−500.

(57) Lednev, I. K.; Ye, T. Q.; Hester, R. E.; Moore, J. N. Femtosecond Time-Resolved UV-Visible Absorption Spectroscopy of *trans*-Azobenzene in Solution. *J. Phys. Chem.* **1996**, *100*, 13338−13341.

(58) Kumita, J. R.; Flint, D. G.; Smart, O. S.; Woolley, G. A. Photo-control of Peptide Helix Content by an Azobenzene Cross-Linker: Steric Interactions with Underlying Residues Are Not Critical. *Protein Eng., Des. Sel.* **2002**, *15*, 561−569.

(59) Culik, R. M.; Abaskharon, R. M.; Pazos, I. M.; Gai, F. Experimental Validation of the Role of Trifluoroethanol as a Nanocrowder. *J. Phys. Chem. B* **2014**, *118*, 11455−11461.

(60) Barua, B.; Lin, J. C.; Williams, V. D.; Kummler, P.; Neidigh, J. W.; Andersen, N. H. The Trp-Cage: Optimizing the Stability of a Globular Miniprotein. *Protein Eng., Des. Sel.* **2008**, *21*, 171−185.

(61) Markiewicz, B. N.; Jo, H.; Culik, R. M.; DeGrado, W. F.; Gai, F. Assessment of Local Friction in Protein Folding Dynamics Using a Helix Cross-Linker. *J. Phys. Chem. B* **2013**, *117*, 14688−14696.

(62) Huang, C.-Y.; Klemke, J. W.; Getahun, Z.; DeGrado, W. F.; Gai, F. Temperature-Dependent Helix−Coil Transition of an Alanine Based Peptide. *J. Am. Chem. Soc.* **2001**, *123*, 9235−9238.

(63) Dyer, R. B.; Gai, F.; Woodruff, W. H.; Gilmanshin, R.; Callender, R. H. Infrared Studies of Fast Events in Protein Folding. *Acc. Chem. Res.* **1998**, *31*, 709−716.

(64) Kennedy, D. F.; Crisma, M.; Toniolo, C.; Chapman, D. Studies of Peptides Forming 3_{10}- and α-Helices and β-Bend Ribbon Structures in Organic Solution and in Model Biomembranes by Fourier Transform Infrared Spectroscopy. *Biochemistry* **1991**, *30*, 6541−6548.

(65) Serrano, A. L.; Tucker, M. J.; Gai, F. Direct Assessment of the α-Helix Nucleation Time. *J. Phys. Chem. B* **2011**, *115*, 7472−7478.

(66) Ihalainen, J. A.; Paoli, B.; Muff, S.; Backus, E. H. G.; Bredenbeck, J.; Woolley, G. A.; Caflisch, A.; Hamm, P. α-Helix Folding in the Presence of Structural Constraints. *Proc. Natl. Acad. Sci. U. S. A.* **2008**, *105*, 9588−9593.

(67) Markiewicz, B. N.; Culik, R. M.; Gai, F. Tightening Up the Structure, Lighting Up the Pathway: Application of Molecular Constraints and Light to Manipulate Protein Folding, Self-Assembly and Function. *Sci. China Chem.* **2014**, *57*, 1615−1624.

(68) Thompson, P. A.; Muñoz, V.; Jas, G. S.; Henry, E. R.; Eaton, W. A.; Hofrichter, J. The Helix-Coil Kinetics of a Heteropeptide. *J. Phys. Chem. B* **2000**, *104*, 378−389.

(69) Lapidus, L. J.; Steinbach, P. J.; Eaton, W. A.; Szabo, A.; Hofrichter, J. Effects of Chain Stiffness on the Dynamics of Loop Formation in Polypeptides. Appendix: Testing a 1-Dimensional Diffusion Model for Peptide Dynamics. *J. Phys. Chem. B* **2002**, *106*, 11628−11640.

(70) Krieger, F.; Fierz, B.; Bieri, O.; Drewello, M.; Kiefhaber, T. Dynamics of Unfolded Polypeptide Chains as Model for the Earliest Steps in Protein Folding. *J. Mol. Biol.* **2003**, *332*, 265−274.

(71) Kubelka, J.; Hofrichter, J.; Eaton, W. A. The Protein Folding 'Speed Limit'. *Curr. Opin. Struct. Biol.* **2004**, *14*, 76−88.

(72) Gruebele, M. Comment on Probe-Dependent and Nonexponential Relaxation Kinetics: Unreliable Signatures of Downhill Protein Folding. *Proteins: Struct., Funct., Bioinf.* **2008**, *70*, 1099−1102.

(73) Liu, F.; Du, D.; Fuller, A. A.; Davoren, J. E.; Wipf, P.; Kelly, J. W.; Gruebele, M. An Experimental Survey on the Transition Between Two-State and Downhill Protein Folding Scenarios. *Proc. Natl. Acad. Sci. U. S. A.* **2008**, *105*, 2369−2374.